Journal of the Neurological Sciences 402 (2019) 40–47

Contents lists available at ScienceDirect

Journal of the Neurological Sciences

journal homepage: www.elsevier.com/locate/jns

Clinical short communication

Diffuse white matter alteration in CLIPPERS: Advanced MRI findings from two cases

Mauro Morassi[a,*], Milena Cobelli[a], Elena Ghiselli[a], Paolo Costa[b], Daniele Bagatto[c], Michela Pievani[d], Claudio Bnà[a]

[a] Department of Radiology, Neuroradiology and Angiology Unit, Fondazione Poliambulanza Istituto Ospedaliero, Via L. Bissolati 57, 25124 Brescia, Italy
[b] Department of Neurology, Fondazione Poliambulanza Istituto Ospedaliero, Via L.Bissolati 57, 25124 Brescia, Italy
[c] Department of Neuroradiology, Azienda Sanitaria Universitaria Integrata di Udine, Presidio Ospedaliero "Santa Maria della Misericordia", Piazzale Santa Maria della Misericordia 15, 33100 Udine, Italy
[d] Lab Alzheimer's Neuroimaging & Epidemiology, IRCCS Istituto Centro San Giovanni di Dio Fatebenefratelli, via Pilastroni 4, 25125 Brescia, Italy

ARTICLE INFO

Keywords:
CLIPPERS
Diffuse tensor imaging
White matter alterations
Susceptibility weighted imaging
Hypointense lesions
Spectroscopy

ABSTRACT

Advanced MRI findings in two patients with probable chronic lymphocytic inflammation with pontine perivascular enhancement responsive to steroids (CLIPPERS) are presented. Diffusion tensor imaging indices (fractional anisotropy and mean diffusivity), evaluated in both patients at baseline MRI examination before treatment and during follow-up, indicated white matter structural changes not only affecting the brainstem, which represents the primary site of inflammatory damage, but also projection (corona radiata) and associative tracts in both patients, while alterations within the corpus callosum were detected in patient 1# at follow-up. Susceptibility weighted imaging (SWI) revealed hypointense lesions in both patients, MRI spectroscopy (MRS) indicated a mildly increased Cho/NAA ratio with no evidence of lipids/lactate peaks, indicating that it may be used as a non-invasive marker to identify CLIPPERS cases suspected for progression to lymphoma.

1. Introduction

Chronic lymphocytic inflammation with pontine perivascular enhancement responsive to steroids (CLIPPERS) is a brainstem-predominant inflammatory disease described in 2010 [1]. Magnetic resonance imaging (MRI) demonstrates a characteristic pattern of perivascular punctate and/or curvilinear foci of gadolinium enhancement typically located in the pons and cerebellum. However, a recent study using ultra-high-field 7T MRI suggests the involvement also of supratentorial structures, indicating a more global cerebral damage than commonly detected by structural 1.5–3 T MRI [2]. Here, we present two cases of probable CLIPPERS according to Tobin et al. criteria [3], evaluated for the first time using diffusion MRI tensor imaging (DTI) with tract-based spatial statistics (TBSS), a technique providing a quantitative evaluation of microstructural tissue damage in inflammatory conditions [4,5]. Specifically, we considered two indices, fractional anisotropy (FA) and mean diffusivity (MD), as measures of microstructural integrity. A decrease in FA is generally considered to reflect axonal loss, while MD is a measure of water molecule random motion that is recognised as a marker of general tissue damage - its increase indicates tissue disruption due to inflammation with increase in extracellular space [6]. DTI indices were evaluated within the brainstem, which represents the primary site of damage in CLIPPERS, and within the major associative/projective tracts, as literature data indicate a neuro-degenerative course with cerebral atrophy and cognitive impairment in some cases [7]. In order to better characterize CLIPPERS abnormalities and to possibly identify features that may distinguish it from others inflammatory diseases, we also investigated FA and MD values within the commissural tracts, particularly the corpus callosum, which is typically involved in multiple sclerosis patients [5,8,9]. Additionally, findings of susceptibility weighted imaging (SWI) and MR spectroscopy (MRS) are described.

1.1. Cases presentation

1.1.1. Case 1#

A 74 years old woman presenting with a one-month history of subacute vertigo, postural instability, bilateral tremor, horizontal diplopia and bilateral tinnitus. Medical history included colon cancer treated with surgery alone (no post-operative chemotherapy or radiotherapy) two years before. An initial out-patient brain MRI without contrast material injection (performed in another institution) showed

* Corresponding author.
E-mail address: mauro.morassi@poliambulanza.it (M. Morassi).

https://doi.org/10.1016/j.jns.2019.04.041
Received 30 December 2018; Received in revised form 26 March 2019; Accepted 30 April 2019
Available online 02 May 2019
0022-510X/ © 2019 Elsevier B.V. All rights reserved.

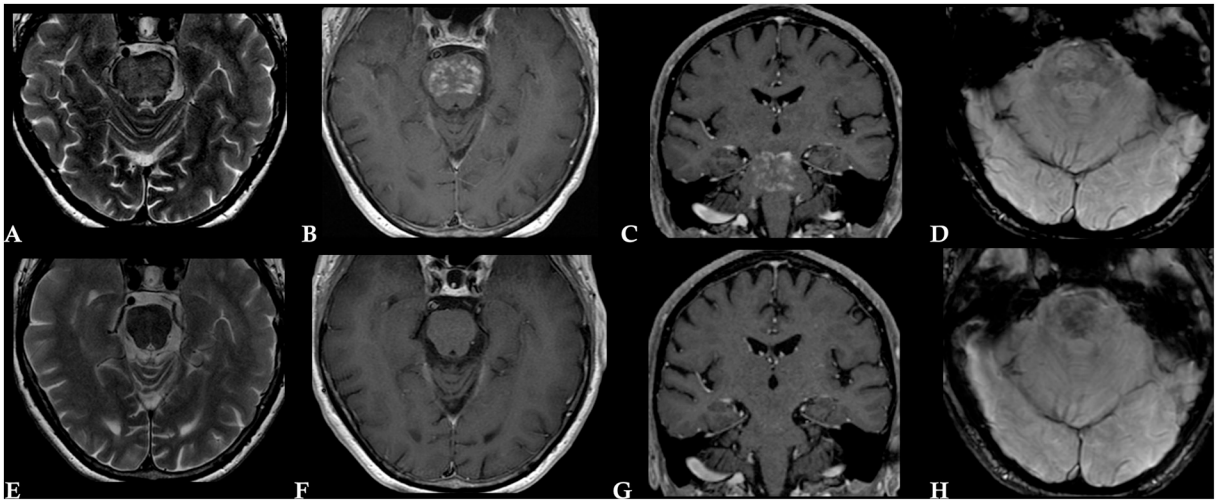

Fig. 1. CLIPPERS Patient 1#. Baseline MRI: multiple small T2 hyperintense lesions in the pons (A) showing prominent punctate, curvilinear enhancements (B–C); few pontine punctate hypointense lesions occurred at SWI. Follow-up MRI at 1 year from presentation: nearly complete resolution of the lesions (E) with only few minimal residual punctate enhancements (F–G) and volumetric reduction of the pons; SWI revealed an hypointense area in the pons (H).

diffuse pontine white matter hyperintensity on T2-weighted images, which was interpreted as osmotic pontine myelinolysis. The neurological examination revealed mild ataxia, horizontal diplopia, increased bilateral deep tendon reflexes (slightly more accentuated on the right side) and hypo-dysesthesia (particularly at the antero-lateral aspect of the leg and foot on the right side). No cranial nerve deficit was observed. Structural MRI of the brain revealed multiple, small T2 hyperintense lesions within the pons, midbrain (cerebral peduncles), inferior cerebellar peduncles, and base of middle cerebellar peduncles with prominent punctate or curvilinear enhancement (Fig. 1A-C). None of the lesions had mass effect. Spinal cord MRI revealed no medullary lesions. Body fludeoxyglucose F18 positron emission tomography and chest-abdomen CT imaging showed normal findings. Blood count (including total leucocyte count), renal and liver function tests, sedimentation rate, electrolytes, c-reactive protein (CRP) and thyroid hormone levels were normal. Tumor markers α-fetoprotein (AFP), Cancer Antigen (CA)-125, Carcinoembryonic antigen (CEA) and carbohydrate antigen (CA) 19-9 were negative. Serological evaluation, including antinuclear antibodies (ANA), extractable nuclear antigen (ENA), Anti-neutrophil cytoplasmic antibodies (ANCA), anti-thyroid peroxidase (TPO), anti-thyreoglobulin, anti GQ1B, anti-aquaporin channel 4 (AQP4), anti-myelin oligodendrocyte glycoprotein (MOG) and onconeuronal antibodies (anti-amphiphysin, anti-Ri, anti-Yo, anti-Hu, anti-CV2, anti-Ma2/Ta), were all negative. Serological testing excluded Epstein-Barr virus, HIV 1-2 and *Borrelia*. CSF examination revealed elevated total proteins (72 mg/dL vs normal range 20–45 mg/dL), albumin (49 mg/dL vs normal <35 mg/dL) and IgG (5.2 mg/dL vs normal range 0.6–3.8 mg/dL) levels while cytology demonstrated a mild lymphocytic pleocytosis (CD3+ lymphocytes 6/mm^3 vs normal <4/mm^3). Oligoclonal bands were absent. The patient was treated for five consecutive days with 1000 mg intravenous methylprednisolone, with symptoms improvement and was discharged with indication to oral steroid therapy (50 mg/die of prednisone) followed by further remarkable improvement of diplopia and gait. The therapy was discontinued seven months later when the inflammatory lesions detected on MRI regressed. An MRI evaluation three months later showed few punctiform enhancements within the brainstem. In consideration of the clinical stability, however, the steroid therapy was not resumed. A subsequent neurological and radiological examination two months later (i.e., 1 year after presentation) demonstrated clinical stability with minimal residual MRI signal alterations (Fig. 1E–G).

1.1.2. Case 2#

A 78-year-old man with one-month history of dysphagia, dysarthria, peri-oral and tongue paraesthesia, trigeminal hypo-paraesthesia affecting the V2 and V3 divisions of the trigeminal nerve on both sides (predominant on the left) and gait impairment within the previous two months. Medical history included bilateral glaucoma, myocardial infarction treated by PTCA, atrial fibrillation, macrocytic anaemia (deficiency of vitamin B12), mild renal insufficiency, vertebral osteoporotic fractures (L1 – L2). Structural MRI revealed symmetrical T2 hyperintense lesions of the bilateral middle cerebellar peduncle, at level of intra-pontine fibers of the trigeminal nerve (Fig. 2A), also involving bilateral inferior cerebellar peduncle. Following contrast material injection, the cerebellar peduncles lesions appeared as ovoid-like areas of enhancement, formed by coalescence of smaller punctate, curvilinear or nodular enhancements with few isolated punctate enhancing lesions within the pons (Fig. 2B-C). Body fludeoxyglucose F18 positron emission tomography and chest-abdomen CT imaging showed normal findings. Brain PET-CT showed moderate hypermetabolism corresponding to the bilateral enhancing areas (SUVmax 7.5). Work-up at admission included complete and differential blood count, renal and liver function tests, sedimentation rate, electrolytes, c-reactive protein (CRP), thyroid hormone levels. The following parameters were found increased: mean corpuscular volume (MCV) (99.1 vs normal range 82–97.00 fL/cell), mean corpuscular haemoglobin (33.5 vs 27–33 pg/cell), creatinine (1.22 vs normal range 0.70–1.20 mg/dL), urea (58 vs normal range 17–49 mg/dL), total bilirubin (1.8 vs normal value <1.2 mg/dL) and direct bilirubin (0.7 vs normal value <0.3 mg/dL), beta2-microglobulin (2.5 mg/L vs 0.8–2.2 mg/L), ferritin (949 ng/mL vs 30–400 ng/mL). A further finding in patient 2# was represented by lymphocytopenia (0.3×10^3/μL vs normal range 0.90–5.00 $\times10^3$/μL). Tumor markers (α-AFP, CA-125, CEA and CA 19-9) were negative. Work up for infectious pathogens (EBV, HIV 1–2 and *Borrelia*), autoimmune antibodies (ANA, ENA, ANCA, anti-TPO, anti-thyreoglobulin, anti-AQP4, anti-MOG) were all negative. CSF examination demonstrated no abnormal finding. Oligoclonal bands were absent.The patient was treated for five consecutive days with 1000 mg intra-venous methylprednisolone followed by oral steroid therapy (50 mg/die of prednisone). The patient's symptoms improved and at follow-up (3 and 6 months from presentation) only mild facial hypoesthesia (particularly on the left side) and mild gait imbalance persisted. MRI examination demonstrated mild residual bilateral T2 hyperintensity with resolution of the enhancing lesions (Fig. 2D-F).

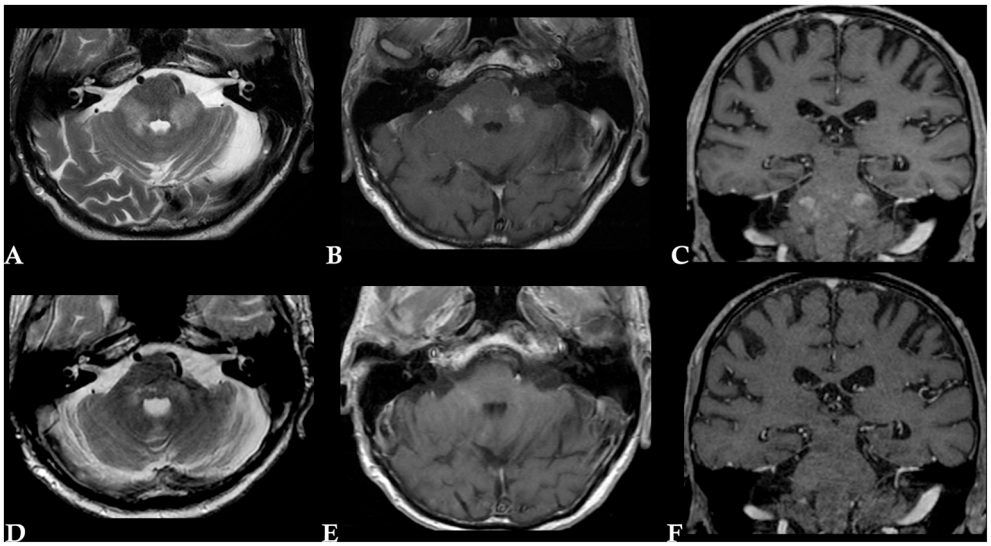

Fig. 2. CLIPPERS Patient 2#. Baseline MRI: symmetrical T2 hyperintense lesions of the bilateral middle cerebellar peduncle (A); following gadolinium injection numerous punctate, curvilinear and nodular coalescent enhancements were noted at level of the hyperintense lesions (B–C). Follow up MRI at six months from presentation demonstrated mild residual symmetrical hyperintense lesions (D) with no enhancement (E–F).

2. Methods

2.1. Structural and advanced MRI data acquisition

MR examinations were obtained from a 1.5 T scanner (Signa Hdxt, GE Medical Systems Milwaukee USA). Structural MR imaging was performed in CLIPPERS patients with multiplanar T2 FSE, 3D FLAIR, DWI SE/EPI, 3D SWI, axial T1 SE pre and post-contrast (Gadolinium) injection (Dotarem, 15 mL), T1 3D SPGR post-contrast. Single-voxel (voxel size: $20 \times 20 \times 20\,mm^3$) proton MRS was performed in the areas of abnormality (pons in patient 1# and base of middle cerebellar peduncle in patient 2#, see Fig. 3A-B) using a PRESS protocol with TR/TE = 1500/144. Intracranial vascular imaging was available for both patients (3D Time-of-Flight MR angiography). Two different diffusion tensor imaging (DTI) protocols were used: patient 1# and 17 healthy controls (HC) underwent an axial single-shot SE/EPI sequence with 24 gradient directions (*b* values: 0 and 1000 s/mm), 5 mm slice thickness, TR/TE = 6000/96.6, FOV 280 × 280 mm, matrix 128 × 128 mm, NEX = 2. Patient 2# and 5 healthy controls (HC) underwent an axial single-shot SE/EPI sequence with 64 gradient directions (b values: 0 and 1000 s/mm), 3 mm slice thickness, TR/TE = 11,625/95.5, FOV 280 × 280 mm, matrix 128 × 128 mm, NEX = 2. Spinal cord MRI was performed with sagittal FSE T2, STIR and post-contrast T1 FSE. Structural MR examinations were obtained at baseline in both patients and during a 1 year follow-up in patient 1# and six months follow-up in patient 2# DTI was acquired at baseline (before treatment) for both patients, at 1 year after presentation (five months after treatment) in patient 1# and six months after commencement of the treatment in

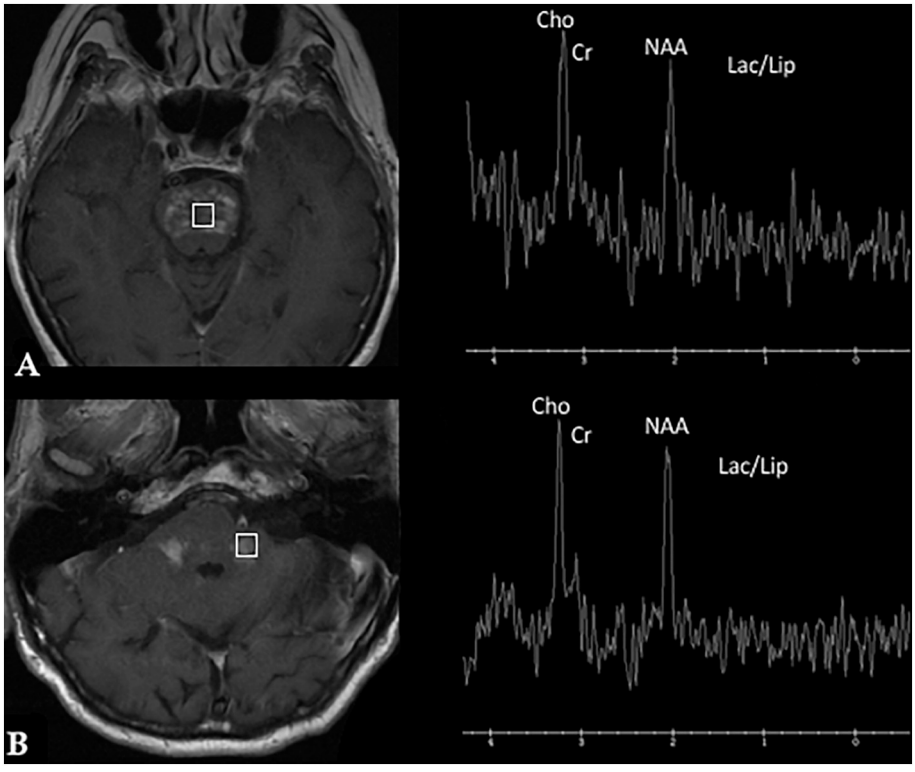

Fig. 3. CLIPPERS Spectroscopy: Patient 1# (A). Patient 2# (B).

patient 2#. Healthy controls were age-matched (73.9 ± 3.6 years) subjects free of neurological, cognitive or psychiatric diseases. The study followed the ethical rules and a written informed consent was obtained from each participant in accordance with the Declaration of Helsinki.

2.2. DTI analysis

Diffusion tensor imaging (DTI) images were corrected for motion and eddy currents with FSL's eddy tool (https://fsl.fmrib.ox.ac.uk/fsl/fslwiki/eddy). The corrected data were then processed with FSL DTIfit tool for the estimation of diffusion indices, fractional anisotropy (FA) and mean diffusivity (MD). Tract-based spatial statistics (TBSS, part of FSL; [10]); http://www.fmrib.ox.ac.uk/fsl/tbss/index.html) was used to non-linearly align all the DTI images to a common reference space. The procedure non-linearly transform each subject's FA to the FMRIB58_FA standard-space FA template using the FMRIB's Non-linear Image Registration Tool (FNIRT, part of FSL). This registration was subsequently applied to the MD maps to project all the diffusivity images onto the standard space.

Regions of interest (ROIs) were defined using the Johns Hopkins University (JHU) white-matter labels atlas (ICBM-DTI-81 white-matter labels atlas; http://fsl.fmrib.ox.ac.uk/fsl/data/atlas-descriptions.html; [11]). The atlas includes 48 ROIs covering the major WM tracts of the brain (Fig. 4). ROIs were classified into brainstem, projection, associative and commissural tracts, as follows. Brainstem tracts were the bilateral cerebellar peduncles (including the inferior - ICP, middle - MCP, superior - SCP, and pontine part - PCP), the bilateral medial lemniscus (ML), the bilateral corticospinal tracts (CST). Projection tracts were the bilateral cerebral peduncles (CP), the bilateral internal capsule (IC - including the anterior, posterior and retro-lenticular part, and the superior fronto-occipital tract), the bilateral corona radiata (CR – including anterior, posterior, and superior portions), the bilateral thalamic radiation (TR). Cortical association tracts included the bilateral cingulum (cingulate and hippocampal parts), the uncinate fasciculus (UF), the external capsule, the superior longitudinal fasciculus (SLF), the sagittal stratum (inferior longitudinal fasciculus and inferior fronto-occipital fasciculus – ILF/IFO). The corpus callosum (including the genu, body, and splenium) was included as commissural tract. All ROIs were back projected to each subject's FA and MD map using the inverse of the nonlinear registration computed with TBSS. The average diffusivity values (FA, MD) within each ROI were then computed in the native space. FA and MD values were computed for each patient and HC. Controls were then used as a reference group to classify patient's diffusivity values as pathological/normal. Specifically, FA and MD scores of each patient were converted into Z scores based on the data distribution of the corresponding HC group. Z scores < -1.96 for FA and Z scores > 1.96 for MD were considered as pathological.

3. Results

3.1. DTI indices

Diffusion values (FA and MD) within brainstem, projection, associative and commissural tracts of patient 1# and patient 2# are reported in Table 1 and Table 2 respectively.

Most brainstem tracts showed pathologically altered indices (FA and/or MD) at baseline (bilateral CST, bilateral ML, MCP, PCP and left inferior ICP in patient 1#; bilateral ML, bilateral ICP and MCP in patient 2#). At follow-up some brainstem tracts with base-line pathological indices reverted to normal ($-1.96 < Z < 1.96$) or showed reduction of the alteration while in other tracts the diffusion indices become pathological (right ICP, left SCP in patient 1#) or showed worsening (MCP and PCP in patient 1#; left ICP in patient 2#).

Projection tracts with pathological indices at baseline (bilateral CP, right CR and right IC in patient 1#; bilateral CR and bilateral TR in patient 2#) did not revert to normal at follow-up (with the exception of left CP in patient 1#). Furthermore, worsening of pathological indices within the right CR and right IC was noted in patient 1#.

In patient 1# DTI indices at base-line were normal within the associative tracts with the exception of the left cingulum and right SLF. At follow-up numerous tracts became pathological (left SLF, right ILF/IFO, right cingulum, right UF), and worsening of the pathological alterations was noted within the left cingulum and right SLF. In patient 2# associative tracts were normal both at base-line and follow-up, except for pathological values noted within the right ILF/IFO which showed worsening at follow-up. No alteration of DTI indices was reported within corpus callosum in patient 2#, while FA became pathological in patient 1# at follow-up.

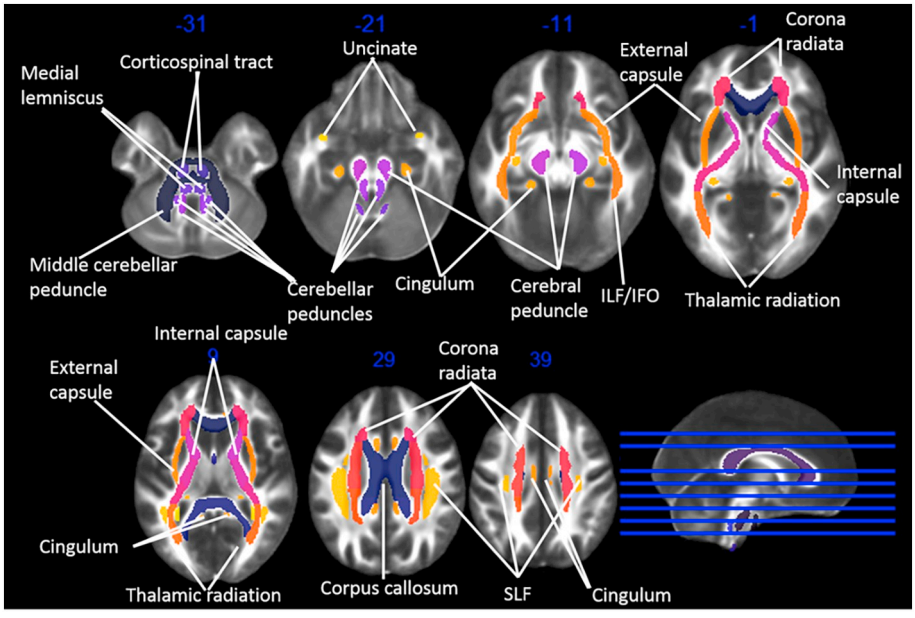

Fig. 4. The JHU atlas with the regions of interest investigated.

Table 1
Fractional anisotropy (FA) and mean diffusivity (MD) values of patient 1#.

WM tract	FA			MD		
	Baseline	Follow-up	Δ	Baseline	Follow-up	Δ
Brainstem tracts						
Corticospinal tract L	**−6.47**	**−2.57**	+35%	**2.33**	1.33	−11%
Corticospinal tract R	**−4.09**	−1.65	+35%	0.79	0.40	−7%
Medial lemniscus L	**−4.22**	**−3.25**	+8%	**7.27**	0.27	−19%
Medial lemniscus R	**−3.52**	**−4.93**	−9%	**5.43**	1.57	−9%
Cerebellar peduncle – inferior L	−1.70	−1.49	3%	**2.69**	0.62	−29%
Cerebellar peduncle – inferior R	−1.54	**−3.03**	−13%	1.50	1.16	−6%
Cerebellar peduncle – middle	**−3.00**	**−3.10**	−1%	0.87	**2.01**	+8%
Cerebellar peduncle – pontine tract	−1.54	**−2.28**	−8%	**2.60**	**2.29**	−2%
Cerebellar peduncle – superior L	−1.77	**−2.20**	−3%	0.62	1.89	+16%
Cerebellar peduncle – superior R	−1.47	−1.31	+1%	0.05	1.08	+13%
Projection tracts						
Cerebral peduncle L	**−4.57**	−0.33	+18%	**3.03**	0.76	−8%
Cerebral peduncle R	**−2.88**	**−2.48**	+2%	1.77	1.55	−1%
Corona radiata L	−1.36	−1.36	0%	1.34	1.77	+3%
Corona radiata R	**−2.00**	**−2.48**	−4%	1.33	**2.12**	+6%
Internal capsule L	−1.21	−1.79	−3%	0.26	1.42	+5%
Internal capsule R	**−2.26**	**−3.16**	−4%	0.43	**2.10**	+6%
Thalamic radiation L	−1.02	−1.60	−6%	0.59	1.47	+8%
Thalamic radiation R	−0.66	−1.09	−4%	0.68	1.44	+5%
Associative tracts						
Cingulum L	−0.84	−1.88	−7%	**2.54**	**3.75**	+3%
Cingulum R	−0.03	**−2.58**	−23%	0.77	**3.40**	+11%
External capsule L	−0.68	−1.00	−2%	−0.16	0.11	+2%
External capsule R	−0.48	−1.26	−5%	0.17	0.54	+3%
SLF L	−1.10	**−2.29**	−9%	1.22	**2.09**	+6%
SLF R	−1.65	**−3.62**	−14%	**2.91**	**3.89**	+5%
ILF/IFO L	−0.82	−1.73	−10%	−0.21	−0.15	+1%
ILF/IFO R	−1.18	**−2.08**	−8%	0.48	0.55	+1%
Uncinate fasciculus L	−1.61	−1.69	−1%	0.53	−0.60	−8%
Uncinate fasciculus R	−1.82	−1.22	+10%	1.00	**2.50**	+7%
Commissural tracts						
Corpus callosum	−1.93	**−2.39**	−2%	0.40	1.76	+9%

Values denote Z scores or changes from baseline (%). Bold values denote abnormal Z scores in patient 1# compared with the control group. IFO: inferior fronto-occipital fasciculus, ILF: inferior longitudinal fasciculus, L: left, R: right, SLF: superior longitudinal fasciculus.

3.2. SWI and MRS findings

In patient 1# SWI showed few punctate hypointensities within the pons at baseline MRI (Fig. 1D), remarkably increasing in number and largely confluent in a distinct hypointense area with ill-defined margins at follow-up. This area corresponded to previous contrast-enhancing lesions and was probably related to extra-vascular iron deposition (Fig. 1H). In patient 2#, SWI demonstrated an intra-lesional lineariform hypointensity within the left middle cerebellar peduncle at base-line, probably related to the increased concentration of deoxygenated blood within a small vein. Conversely, a faint hypointensity with ill-defined margin detected at the same level six months after presentation was more probably related to iron deposition due to the chronic course of local inflammation.

MR spectroscopy findings were very similar in both patients with a slightly elevated Cho/NAA ratio (1–1.12) but no evidence of lipids/lactates peaks (Fig. 3A–B).

4. Discussion

Since 2010, numerous CLIPPERS cases have been reported and the typical clinical scenario, neuroradiological features and steroid response have been quite well defined. CLIPPERS pathogenesis and nosological position are only partially known, but current data suggest a central role of complement activation with endothelial damage, perivascular deposition of IgG in vessels and inflammatory infiltrates predominantly composed of CD4+ T cells [12].

Tobin et al., 2017 recently proposed diagnostic criteria for CLIPPERS, but numerous cases challenging their proposed criteria have been described, including cases of a pontine sparing CLIPPERS "variant", for which the term "Supratentorial Lymphocytic Inflammation with Parenchymal Perivascular Enhancement Responsive to Steroids (SLIPPERS)" has been proposed [13–16].

According to the recently proposed diagnostic criteria, a "definite" diagnosis of CLIPPERS can be proposed only when histopathological data are available [3]. However, it has been suggested that, given the location of CLIPPERS lesions within the brainstem, brain biopsy should be performed in cases when alternative diagnoses remain likely despite complete clinical, laboratory and imaging assessment [1,17]. The two patients discussed here met the clinical-radiological features of CLIPPERS and other alternative diagnoses have been ruled out; for these reasons, they are here presented as "probable" CLIPPERS cases. Patient 1# had an history of colon cancer and the possibility of a para-neoplastic brainstem encephalitis, in particular associated with anti-Hu antibodies [18] has been considered. However, the patient was negative for onco-neural antibodies (including anti-Hu) and the clinical-radiological improvement with therapy do not support a paraneoplastic syndrome. Patient 2# showed small coalescent lesions forming bilateral ovoid enhancing areas at level of intra-pontine fibers of the trigeminal nerves. According to Tobin et al. criteria the enhancing area should not exceed 3 mm in diameter. However, in numerous CLIPPERS cases enhancing lesions may show, at least focally, a tendency to confluence (see, for example, case 2 figured by Simon et al. [7]). Even in the original case series discussed by Pittock et al., 2010 the diameter of the enhancing lesions was stated to vary between 1 and 3 mm up to 9 mm.

A bilateral involvement of the intra-pontine fascicular part of the

Table 2
Fractional anisotropy (FA) and mean diffusivity (MD) values of patient 2#.

WM tracts	FA			MD		
	Baseline	Follow-up	Δ	Baseline	Follow-up	Δ
Brainstem tracts						
Corticospinal tract L	−1.54	−0.43	+10%	−0.21	0.41	+7%
Corticospinal tract R	−0.20	0.72	+9%	−0.65	−0.35	+4%
Medial lemniscus L	**−2.50**	−0.84	+12%	**2.47**	0.76	−9%
Medial lemniscus R	**−4.41**	−1.46	+26%	**4.31**	0.53	−23%
Cerebellar peduncle – inferior L	**−2.63**	**−3.89**	−5%	−0.73	−0.72	<1%
Cerebellar peduncle – inferior R	**−2.11**	−1.47	+15%	−0.06	−0.45	−9%
Cerebellar peduncle – middle	**−2.28**	−1.03	+11%	1.29	0.46	−8%
Cerebellar peduncle – pontine tract	−0.42	1.12	+15%	−0.82	0.44	+7%
Cerebellar peduncle – superior L	0.51	0.70	+2%	−0.41	−0.47	−1%
Cerebellar peduncle – superior R	−0.19	−0.11	+1%	−0.34	0.33	+11%
Projection tracts						
Cerebral peduncle L	−0.44	−0.40	<1%	1.35	0.83	−3%
Cerebral peduncle R	−0.68	−0.84	−1%	0.77	0.98	+1%
Corona radiata L	**−2.09**	**−2.18**	−1%	0.17	0.28	+1%
Corona radiata R	**−1.96**	**−1.96**	0%	0.20	0.36	+1%
Internal capsule L	−0.63	−0.63	0%	0.09	0.09	0%
Internal capsule R	−0.97	−0.77	+1%	0.57	0.29	−2%
Thalamic radiation L	**−2.81**	**−2.79**	0%	**2.51**	**2.39**	−1%
Thalamic radiation R	**−2.77**	**−3.16**	−4%	1.31	1.72	+4%
Associative tracts						
Cingulum L	−0.65	−1.04	−4%	0.05	1.09	+6%
Cingulum R	−0.94	−0.66	+2%	0.78	0.17	−4%
External capsule L	0.70	0.61	<1%	0.34	0.11	−1%
External capsule R	0.31	−0.38	−3%	−0.07	0.22	+2%
SLF L	−1.25	−1.14	+1%	0.13	0.29	+1%
SLF R	−1.06	−1.42	−3%	−0.41	−0.24	+1%
ILF/IFO L	−1.37	−0.81	+3%	0.43	0.20	−3%
ILF/IFO R	**−2.67**	**−2.96**	−2%	1.88	**2.04**	+1%
Uncinate fasciculus L	1.39	0.96	−5%	−0.04	1.04	+4%
Uncinate fasciculus R	0.43	0.11	−3%	0.07	−0.10	−2%
Commissural tracts						
Corpus callosum	−0.08	−0.15	<1%	−0.27	−0.26	<1%

Values denote Z scores or changes from baseline (%). Bold values denote abnormal Z scores in patient 2# compared with the control group. IFO: inferior fronto-occipital fasciculus, ILF: inferior longitudinal fasciculus, L: left, R: right, SLF: superior longitudinal fasciculus.

trigeminal nerve has been reported in a CLIPPERS autopsy case [19]. However, trigeminal REZ involvement has been also reported in different demyelinating diseases such MS, NMO and MOG-IgG associated brainstem encephalitis [20], but patient 2# did not met the diagnostic criteria of these conditions. A remarkable laboratory feature of patient 2# is lymphocytopenia which, as far as we known, has previously been reported in a single CLIPPERS case [21]. We follow previous authors [22] in considering the significance of this finding unclear.

Brain 18F-FDG PET/CT was performed in patient 2# and showed increased metabolism at level of the symmetrical areas of enhancement. Data regarding 18F-FDG PET/CT in CLIPPERS patients are restricted to few cases where findings vary from no significant change from normal tissue to hypermetabolism [3,7]. The role of brain PET/CT in CLIPPERS has been considered limited [22,23] but, given the few studied cases, its potential role as a diagnostic tool in the differential diagnosis between CLIPPERS and its mimicks is, in our opinion, still undefined.

Neuropathological data from previous CLIPPERS studies indicate that axonal injury and myelin loss prevail in those brainstem areas where inflammation is more severe, while preservation of axons and myelin occur in areas with more limited inflammation [19].

As expected from structural MRI, brainstem tracts showed pathological DTI indices in both our patients in agreement with clinical findings. In patient 1# the markedly altered DTI indices within bilateral CST may account for the hyperactive bilateral deep tendon reflexes, while the reported sensory alterations (hypo-dysestesia) may be related to the severe pathological alterations of the medial lemniscus. The markedly reduced FA within these tracts suggest the presence of axonal damage as indicated by histopathological evidence [19].

In patient 2#, who was characterized by more circumscribed alterations, DTI indices were pathological within the medial lemniscus in agreement with sensory alterations. Normal DTI values occurred within the bilateral CST and no hyperreflexia was reported in this patient. Pyramidal tracts involvement may therefore not be necessarily present in CLIPPERS patients, as also suggested by a recent CLIPPERS case presenting with trigeminal neuropathy in the absence of any symptoms or signs of brainstem involvement [24]. In both patients reduction of the degree of pathological alteration or reversal to normal values of DTI indices was associated with clinical improvement.

Cerebellar peduncles are another primary site of inflammatory involvement in CLIPPERS and diffusion indices were found altered in both patients, particularly at the level of the middle cerebellar peduncle. CLIPPERS syndrome is characterized by a relapsing-remitting course and histopathological findings indicate variable degree of gliosis and inflammation with or without axonal damage [19]. The variability of DTI indices noted within the cerebellar peduncles in our two patients probably reflects the presence of lesions in different stages of evolution. In patient 1#, diffusion indices within the cerebellar peduncles (particularly MCP and PCP) showed worsening from baseline to follow-up examination due probably to a degenerative course of the disease, in agreement with the clear signs of ponto-cerebellar atrophy noted at conventional MRI examination 1 year after the presentation (compare Fig. 1A-B with Fig. 1E-F).

Blaabjerg et al. (2016) [2], using a 7T MRI scanner, have recently demonstrated in two CLIPPERS patients signs of perivascular inflammation in supratentorial areas with normal appearance on lower field strengths, suggesting a broad brain white matter involvement. In

agreement with this consideration, diffusion imaging findings in our patients demonstrated involvement of numerous white matter tracts during the course of the disease, affecting both the projective and the associative tracts.

The decreased FA values noted within the bilateral posterior thalamic radiation in patient 2# may be the result of the inflammatory process, as reported in multiple sclerosis [5], but the possibility that this alteration is, at least partially, related to the bilateral glaucoma cannot be excluded [25]. Interestingly, diffusion indices within some projective tracts (in patient 1#) and associative tracts (in both patients) became pathological from baseline to follow-up examinations. These alterations probably reflect a neuro-degenerative course of the disease, as suggested by previous reports of cerebral atrophy and/or cognitive impairment in CLIPPERS cases [7–14].

CLIPPERS-like findings in patients with multiple sclerosis have been reported [26,27]. Numerous studies indicate that in multiple sclerosis the white matter is widely altered from the early stage of the disease and the corpus callosum is a typical site of involvement [5,8,9]. In the two patients here discussed, DTI indices were normal within the corpus callosum at baseline examination, while FA values become pathological at follow-up in patient 1# (though, the baseline values were borderline and the overall amount of change $<5\%$). These findings suggest that the corpus callosum is not a primary site of involvement in our CLIPPERS cases and the borderline values noted in patient 1# are more probably the result of the neuro-degenerative course of the disease rather than a direct inflammatory damage.

Altogether, our DTI findings strengthen the concept that CLIPPERS syndrome is characterized by a widespread damage of brain white matter even in areas with no signal alterations at 1.5–3 Tesla MRI, in analogy to multiple sclerosis where structural imaging findings demonstrate only a part of the actual tissue damage.

For a better definition of CLIPPERS syndrome imaging features and their potential pathophysiologic meaning, we have also considered imaging findings from SWI, which allows visualization of venous structures and iron in the brain [28]. SWI has previously been used in a single CLIPPERS case showing multiple hypointense lesions and prominent veins within the brainstem and cerebellum [29]. SWI hypointensities have also been reported in other inflammatory diseases such as multiple sclerosis and neuro-Behçet disease [30,31]. These signal alterations have been related to iron accumulation due to microbleeds (hemorragic transformation of venous micro-infarctions) or chronic inflammation (myelin and/or oligodendrocyte debris) [31,32]. It has also been speculated that in multiple sclerosis patients the iron in microglia cells might propagate chronic, low-grade inflammation, promote neurodegeneration and disease progression [33]. Similar considerations may probably be pertinent for the brainstem damage in CLIPPERS, but the absence of hypointense lesions in the supra-tentorial structures in patients studied with SWI suggest a different mechanism for the white matter damage in these areas.

A major concern in CLIPPERS patients is the reported possibility of progression to lymphoma, which induced some authors to strongly recommend brain biopsy in all CLIPPERS patients [34]. To date, progression to B-cell lymphoma has been reported in four cases on over more one hundred reported [34–37]. Limousin et al., 2012 have reported the presence of MRS peaks in the region of lipids and lactate in a CLIPPERS-like case with subsequent progression to lymphoma, but remarked that the spectroscopic profile in CLIPPERS has not been investigated. MRS findings in both our patients indicate an increased Cho/NAA ratio (1–1.12), which is remarkably lower that reported in neoplastic processes (>1.72 according to Ikeguchi et al., 2018) but somewhat comparable to the values reported in tumefactive demyelinating lesions [38]. No lipids/lactate peaks was detected, thus suggesting that this feature, when present, may lead to suspect the possibility of neoplastic progression. However, some authors have pointed out the limitation of MR spectroscopy in differentiation between neoplastic lesions from inflammatory diseases [39,40]. MRS should therefore be considered a useful tool but only part of the overall judgement on the clinico-radiological data of the patient.

The obvious limitations of the present evaluation derive from the fact that CLIPPERS diagnosis in both patients was not confirmed by histopathological examination. DTI data were collected in only two patients with different acquisition and using a 1.5 T scanner, which is less sensitive than 3 T. Furthermore, no cognitive assessment was conducted with regard to diffusion indices alterations. However, a point of strength is that DTI analysis was performed before patients started the treatment.

Declarations of interest

None.

References

[1] S.J. Pittock, J. Debruyne, K.N. Krecke, et al., Chronic lymphocytic inflammation with pontine perivascular enhancement responsive to steroids (CLIPPERS), Brain 133 (9) (2010) 2626–2634.

[2] M. Blaabjerg, K. Ruprecht, T. Sinnecker, et al., Widespread inflammation in CLIPPERS syndrome indicated by autopsy and ultra-high-field 7T MRI, Neurol. Neuroimmunol. Neuroinflamm. 3 (2016) e226.

[3] W.O. Tobin, Y. Guo, K.N. Krecke, et al., Diagnostic criteria for chronic lymphocytic inflammation with pontine perivascular enhancement responsive to steroids, Brain 140 (2017) 2415–2425.

[4] B. Bodini, Z. Khaleeli, M. Cercignani, et al., Exploring the relationship between white matter and gray matter damage in early primary progressive multiple sclerosis: an in vivo study with TBSS and VBM, Hum. Brain Mapp. 30 (9) (2009) 2852–2861.

[5] S.D. Roosendaal, J.J. Geurts, H. Vrenken, et al., Regional DTI differences in multiple sclerosis patients, Neuroimage 44 (4) (2009) 1397–1403.

[6] E. Sbardella, F. Tona, N. Petsas, et al., DTI measurements in multiple sclerosis: evaluation of brain damage and clinical implications, Mult. Scler. Int. 671730 (2013) 1–11.

[7] N.G. Simon, J.D. Parratt, M.H. Barnett, et al., Expanding the clinical, radiological and neuropathological phenotype of chronic lymphocytic inflammation with pontine perivascular enhancement responsive to steroids (CLIPPERS), J. Neurol. Neurosurg. Psychiatry 83 (1) (2012) 15–22.

[8] T. Sigal, M. Shmuel, D. Mark, et al., Diffusion tensor imaging of Corpus callosum integrity in multiple sclerosis: correlation with disease variables, J. Neuroimaging 22 (2012) 33–37.

[9] A. Pokryszko-Dragan, A. Banaszek, M. Nowakowska-Kotas, et al., Diffusion tensor imaging findings in the multiple sclerosis patients and their relationships to various aspects of disability, J. Neurol. Sci. 391 (2018) 127–133.

[10] S.M. Smith, M. Jenkinson, H. Johansen-Berg, et al., Tract-based spatial statistics: voxel-wise analysis of multi-subject diffusion data, Neuroimage 31 (4) (2006) 1487–1505.

[11] S. Mori, K. Oishi, H. Jiang, et al., Stereotaxic white matter atlas based on diffusion tensor imaging in an ICBM template, Neuroimage 40 (2) (2008) 570–582.

[12] M. Blaabjerg, A.L. Hemdrup, L. Drici, et al., Omics-based approach reveals complement-mediated inflammation in chronic lymphocytic inflammation with pontine perivascular enhancement responsive to steroids (CLIPPERS), Front. Immunol. 9 (2018) 741.

[13] C. Armand, J. Graber, F. Lado, et al., SLIPPERS: Supratentorial lymphocytic inflammation with parenchymal perivascular enhancement responsive to steroids: a case report (P5.118), Neurology 84 (14 Supplement) (2015).

[14] S. Horng, J. Crary, M. Fabian, A case of SLIPPERS (supratentorial lymphocytic inflammation with parenchymal perivascular enhancement responsive to steroids) presenting with isolated cognitive dysfunction. (P1.336), Neurology 88 (16 Supplement) (2017).

[15] S. Okune, K. Ishii, S. Ouchi, et al., A cerebral phenotype of chronic lymphocytic inflammation with pontine perivascular enhancement responsive to steroids: a case report and review of the literature, Mult. Scler. Relat. Disord. 20 (2018) 159–163.

[16] R. Rössling, D. Pehl, M. Lingnau, et al., A case of CLIPPERS challenging the new diagnostic criteria, Brain 141 (2) (2018) 1–3 (e12).

[17] Duprez TP, Sindic CJ. Contrast-enhanced magnetic resonance imaging and perfusion-weighted imaging for monitoring features in severe CLIPPERS. Brain 211, 134: 1–3.

[18] A. Saiz, J. Bruna, P. Stourac, et al., Anti-Hu-associated brainstem encephalitis, J. Neurol. Neurosurg. Psychiatry 80 (2009) 404–407.

[19] I. Moreira, C. Cruto, C. Correia, et al., Chronic lymphocytic inflammation with pontine perivascular enhancement responsive to steroids (CLIPPERS) post-mortem findings, J. Neuropathol. Exp. Neurol. 74 (2015) 186–190.

[20] Y. Shen, Z. Cheng, Chenguang Zhou, Bilateral trigeminal root entry zone enhancement in MOG-IgG-associated brainstem encephalitis, Neurol. Sci. (2018), https://doi.org/10.1007/s10072-018-3668-8.

[21] List J. List, A. Lesemann, E. Wiener, et al., A new case of chronic lymphocytic inflammation with pontine perivascular enhancement responsive to steroids, Brain 134 (8) (2011) e185.

[22] A. Dudesek, F. Rimmele, S. Tesar, et al., CLIPPERS: chronic lymphocytic inflammation with pontine perivascular enhancement responsive to steroids. Review of an increasingly recognized entity within the spectrum of inflammatory central nervous system disorders, Clin. Exp. Immunol. 175 (2014) 385–396.
[23] D. Tian, X. Zhu, R. Xue, et al., Case 259: primary central nervous system Lymphomatoid granulomatosis mimicking chronic lymphocytic inflammation with pontine perivascular enhancement responsive to steroids (CLIPPERS), Radiology 289 (2) (2018) 572–577.
[24] S. Bobba, M. Narasimhan, A. Zagami, Isolated painful trigeminal neuropathy as an unusual presentation of chronic lymphocytic inflammation with pontine perivascular enhancement responsive to steroids: a case report, Cephalalgia (2018) 1–7.
[25] F.G. Garaci, F. Bolacchi, A. Cerulli, et al., Optic nerve and optic radiation neurodegeneration in patients with Glaucoma: in vivo analysis with 3-T diffusion-tensor MR imaging, Radiology 252 (2) (2009) 496–501.
[26] M.R. Ortega, N. Usmani, C. Parra-Herran, et al., CLIPPERS complicating multiple sclerosis causing concerns of CLS lymphoma, Neurology 79 (2012) 715–716.
[27] R.M. Ferreira, G. Machado, A.S. Souza, et al., CLIPPERS-like MRI findings in a patient with multiple sclerosis, J. Neurol. Sci. 327 (1–2) (2013) 61–62.
[28] S. Mittal, Z. Wu, J. Neelavalli, et al., Susceptibility-weighted imaging: technical aspects and clinical applications, part 2, Am. J. Neuroradiol. 30 (2) (2009) 232–252.
[29] I. Pesaresi, M. Sabato, I. Desideri, et al., 3.0 T MR investigation of CLIPPERS: role of susceptibility weighted and perfusion weighted imaging, Magn. Reson. Imaging 31 (2013) 1640–1642.
[30] E.M. Haacke, M. Makki, Y. Ge, et al., Characterizing iron deposition in multiple sclerosis lesions using susceptibility weighted imaging, J. Magn. Reson. Imaging 29 (3) (2009) 537–544.
[31] S. Albayram, S. Saip, Z.I. Hasiloglu, et al., Evaluation of parenchymal neuro-Behçet disease by using susceptibility-weighted imaging, Am. J. Neuroradiol. 32 (6) (2011) 1050–1055.
[32] R. Zivadinov, B. Weinstock-Guttman, I. Pirko, Iron deposition and inflammation in multiple sclerosis. Which one comes first? BMC Neurosci. 12 (2011) 60.
[33] S. Hametner, I. Wimmer, L. Haider, et al., Iron and neurodegeneration in the multiple sclerosis brain, Ann. Neurol. 74 (6) (2013) 848–861.
[34] N. Limousin, J. Praline, O. Motica, et al., Brain biopsy is required in steroid-resistant patients with chronic lymphocytic inflammation with pontine perivascular enhancement responsive to steroids (CLIPPERS), J. Neuro-Oncol. 107 (1) (2012) 223–224.
[35] H.J. De Graaff, M.P. Wattjes, A.J. Rozemuller-Kwakkel, et al., Fatal B-cell lymphoma following chronic lymphocytic inflammation with pontine perivascular enhancement responsive to steroids, JAMA Neurol. (2013) 1–4.
[36] A.W. Lin, S. Das, J.A. Fraser, et al., Emergence of primary CNS lymphoma in a patient with findings of CLIPPERS, Can. J. Neurol. Sci. 41 (2014) 528–529.
[37] G. Taieb, E. Uro-Coste, M. Clanet, et al., A central nervous system B-cell lymphoma arising two years after initial diagnosis of CLIPPERS, J. Neurol. Sci. 344 (1–2) (2014) 224–226.
[38] R. Ikeguchi, Y. Shimizu, K. Abe, et al., Proton magnetic resonance spectroscopy differentiates tumefactive demyelinating lesions from gliomas, Mult. Scler. Relat. Disord. 26 (2018) 77–84.
[39] L.A. Brandão, M. Castillo, Adult brain tumors: clinical applications of magnetic resonance spectroscopy, Magn. Reson. Imaging Clin. N. Am. 24 (4) (2016) 781–809.
[40] A. Vogrig, B. Joubert, F. Ducray, et al., Glioblastoma as differential diagnosis of autoimmune encephalitis, J. Neurol. 265 (3) (2018) 669–677.